Chaos, Solitons and Fractals 117 (2018) 269–275

Contents lists available at ScienceDirect

Chaos, Solitons and Fractals

Nonlinear Science, and Nonequilibrium and Complex Phenomena

journal homepage: www.elsevier.com/locate/chaos

Frontiers

Characteristics of noise-induced intermittency

Olga I. Moskalenko[a,*], Alexey A. Koronovskii[a], Maksim O. Zhuravlev[a], Alexander E. Hramov[a,b]

[a] Saratov State University, Astrakhanskaya, 83, Saratov 410012, Russia
[b] Saratov State Technical University, Politehnicheskaya, 77, Saratov 410054, Russia

ARTICLE INFO

Article history:
Received 8 May 2018
Revised 15 October 2018
Accepted 4 November 2018

Keywords:
Noise
Intermittency
Bistable systems
Residence time distribution

ABSTRACT

We reveal the main characteristics of noise-induced intermittency in a dynamical system with two coexisting attractors. Both the residence time distributions and the mean residence time versus an asymmetry parameter, are found analytically, for each of the coexisting states, and both of them obey exponential laws. The proposed theory is applied to a bistable energy model, dissipatively coupled logistic maps and bistable Chua generator.

1. Introduction

Intermittency is an ubiquitous phenomenon in nonlinear science [1]. It is usually understood as the alternation of apparently regular (periodic or steady state) and irregular (chaotic) behaviors, or the alternation of different chaotic regimes. The initially revealed type of intermittency is known as Pomeau–Manneville dynamics [2], while the latter is called crisis-induced intermittency [3]. Intermittent switches between synchronous and asynchronous behaviors can also occur near the onset of synchronization in a coupled chaotic system. This type of intermittency is referred to as *intermittent synchronization* (see, e.g. [4–9]).

Intermittency is observed in diverse dynamical systems, including physical, medical and biological ones (see, e.g., [10–16]). Several types of intermittent dynamics are traditionally classified into types I–III [1,17], on–off [18], eyelet [4,13], and ring [7] intermittencies, as well as mixed intermittency types can be released [19–21]. Among the different kinds of intermittent chaotic synchronization, one can distinguish intermittent generalized synchronization [6], intermittent lag synchronization [5], intermittent phase synchronization [22,23], etc., depending on the type of the synchronous regime. Each intermittency type is known to be characterized by specific mechanisms and statistical properties which unambiguously allow the determination of the intermittency type taking place in the system. Intermittency is typically characterized by the distribution of laminar phase lengths calculated at the fixed control parameters and the dependence of the mean laminar phase length on a criticality parameter.

Recently, the notion of intermittency was extended to multistable systems, where noise induces switches between coexisting states. In this case, the system is said to demonstrate *noise-induced intermittency*, also known as *multistate intermittency* [24,25] or attractor hopping [26–30]. Correspondingly, instead of *laminar phases* the concept of *residence times* is used, i.e., time intervals when the system is in the vicinity of one of the coexisting states without switching between them. As a consequence, for noise-induced multistate intermittency, the residence time distribution and the dependence of the mean residence time on a criticality parameter should be considered as statistical characteristics of this kind of intermittency.

Despite of some achievements in the study of noise-induced intermittency (see, e.g. [30–36]), there still remains a number of problems demanding consideration and discussion. One of them is the lack of an appropriate theory (except for special cases [33–36]) which would reveal the main characteristics of noise-induced intermittency, including the case of a bistable dynamical system.

The aim of this work is to develop a quantitative theory of noise-induced intermittency in a system with two coexisting regimes, and prove it with several different systems, from the point of view of the proposed theory comparing the statistical characteristics of the behavior of these systems with the theoretical predictions.

The paper is organized as follows. In Section 2 we introduce the general theory of noise-induced intermittency for systems with two coexisting regimes. In Section 3 we prove our theory with the

* Corresponding author.
E-mail address: o.i.moskalenko@gmail.com (O.I. Moskalenko).

https://doi.org/10.1016/j.chaos.2018.11.001
0960-0779/

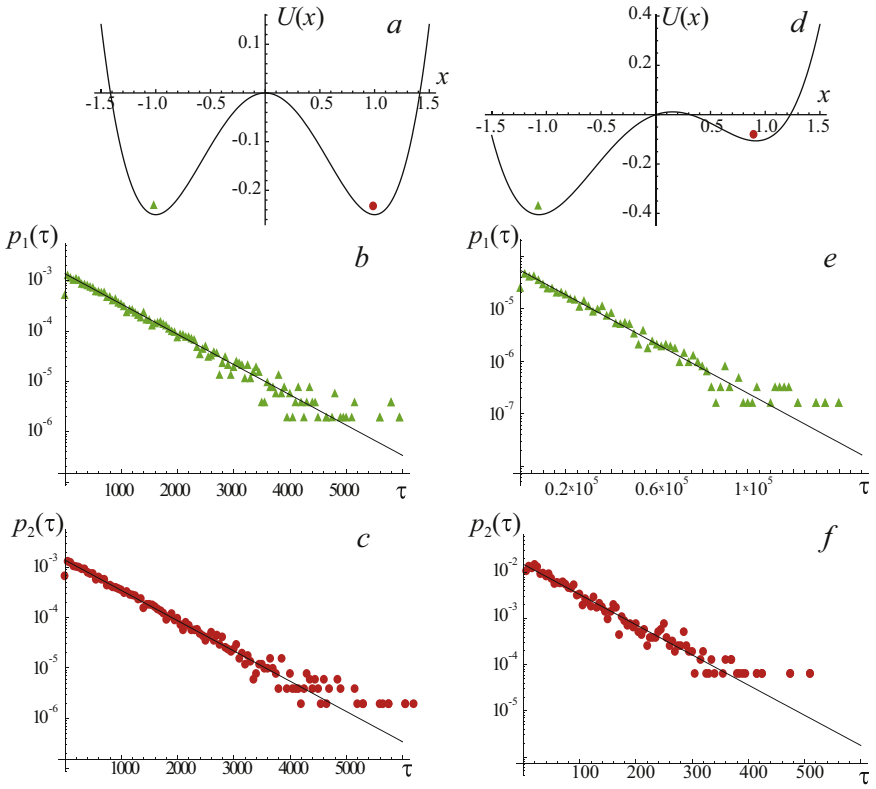

Fig. 1. (Color online) (a,d) Potential functions and (b,c,e and f) residence time distributions for two coexisting regimes in bistable energy model Eq. (1) for two different values of the asymmetry parameter (a–c) $b = 0$ and (d–f) $b = 0.15$. Signs and straight lines show respectively the results of the numerical calculations and theoretical approximations by the regularity Eq. (22), using the following approximation parameters: (b) $T_1 = 722$, (c) $T_2 = 722$, (e) $T_1 = 18508$, and (f) $T_2 = 66$.

examples of a bistable energy model, two mutually coupled logistic maps and bistable Chua generator. The main conclusions are given in Section 4.

2. Theory of noise-induced intermittency

A universal bistable system capable of demonstrating noise-induced intermittency can be written as

$$\frac{dx}{dt} = -\frac{dU(x)}{dx} + \xi(t), \tag{1}$$

where $\xi(t)$ is zero mean δ-correlated Gaussian noise [$\langle \xi(t) \rangle = 0$, $\langle \xi(t)\xi(\tau) \rangle = D\delta(t-\tau)$], and D is the noise intensity. The dimensionless energy function

$$U(x) = \frac{x^4}{4} - \frac{x^2}{2} + bx \tag{2}$$

is shown in Fig. 1(a). It has two local minima $x_{1,2}$ ($U'(x_{1,2}) = 0$, $U''(x_{1,2}) > 0$) separated by the unstable equilibrium x^* ($U'(x^*) = 0$, $U''(x^*) < 0$) corresponding to the local maximum of $U(x)$. $|b| < 2/(3\sqrt{3})$ is the parameter of the asymmetry of the potential [37–41]. In the noiseless system ($D = 0$) the stable fixed points $x_{1,2}$ correspond to two states of the bistable system, whereas in the presence of noise ($D > 0$) two areas: $-\infty < x < x^*$ and $x^* < x < +\infty$, separated by x^* are associated with the rival coexisting regimes. In fact, Eqs. (1) and (2) represent the universal model which describes the bistable system dynamics, since the diversity of bistable energy functions can be reduced to the fourth-degree polynomial in the form of Eq. (2) [42].

The differential Eq. (1) with stochastic term $\xi(t)$ results in the stochastic differential equation

$$dX = -\frac{dU(x)}{dx}\,dt + dW, \tag{3}$$

(where $X(t)$ is a stochastic process and $W(t)$ is a one-dimensional Winner process), equivalent to the Fokker–Planck equation

$$\frac{\partial \rho_X(x,t)}{\partial t} = \frac{\partial}{\partial x}\left[\frac{dU(x)}{dx}\rho_X(x,t)\right] + \frac{D}{2}\frac{\partial^2 \rho_X(x,t)}{\partial x^2} \tag{4}$$

for the probability density $\rho_X(x, t)$ of the stochastic process $X(t)$.

Statistical characteristics of the system behavior, namely, the residence time distribution and the dependence of the mean residence times on the control parameters can be obtained from the evolution of the probability densities $\rho_{1,2}(x, t)$ for both coexisting states separately, i.e., $\rho_1(x, t)$ at $I_1 = -\infty < x < x^*$ and $\rho_2(x, t)$ at $I_2 = x^* < x < +\infty$. Both probability densities $\rho_{1,2}(x, t)$ must obey the Fokker–Planck Eq. (4) in their definitional domains $I_{1,2}$.

Since in the intermittency regime the coordinate of the system state is in the vicinity of one of the local minima for a long time, we can assume that the probability densities $\rho_{1,2}(x, t)$ can be found in the form of the metastable distribution, slowly decaying for a long period of time, i.e.

$$\rho_{1,2}(x,t) = A_{1,2}(t)r(x), \tag{5}$$

where $r(x)$ is the stationary probability density obtained from the solution of Eq. (4) in the stationary case and $A_{1,2}(t)$ are the coefficients slowly decreasing in time.

The general form of the stationary probability density $r(x)$ being the solution of the Fokker–Planck Eq. (4) can be obtained (see [43]) as

$$r(x) = \exp\left(-\frac{2U(x)}{D}\right)\left[C_1 + C_2\int_0^x \exp\left(\frac{2U(\xi)}{D}\right)d\xi\right]. \tag{6}$$

Having found the constant C_2 from the extremum condition

$$r'(x_{1,2}) = C_2 = 0, \tag{7}$$

we get the final form of the stationary probability density function

$$r(x) = C_1 \exp\left(-\frac{2U(x)}{D}\right), \tag{8}$$

where C_1 can be found from the normalization condition

$$\int_{-\infty}^{+\infty} r(x)\,dx = 1. \tag{9}$$

Finally, the stationary probability density $r(x)$ can be expressed in the form

$$r(x) = \frac{g(x)}{\int_{-\infty}^{\infty} g(\xi)d\xi}, \tag{10}$$

where

$$g(\xi) = \exp\left(-\frac{2U(\xi)}{D}\right). \tag{11}$$

The explicit form for the function $A(t)$ can be, in turn, derived from the differential equation

$$\frac{dA_{1,2}}{dt} = -\frac{k}{P_{1,2}} A_{1,2}(t) r(x^*), \tag{12}$$

where x^* is the critical point separating two coexisting states of the bistable system Eqs. (1) and (2), k is a proportionality factor, and $P_{1,2}$ are the probabilities for the representation point to be located in the vicinity of the first or the second local minimum, respectively, defined as

$$\begin{aligned} P_1 &= \int_{-\infty}^{x^*} r(\xi)\,d\xi = \frac{\int_{-\infty}^{x^*} g(\xi)d\xi}{\int_{-\infty}^{+\infty} g(\xi)d\xi}, \\ P_2 &= \int_{x^*}^{+\infty} r(\xi)\,d\xi = \frac{\int_{x^*}^{+\infty} g(\xi)d\xi}{\int_{-\infty}^{+\infty} g(\xi)d\xi}. \end{aligned} \tag{13}$$

In the limit of a large potential barrier in comparison with the noise intensity $A_{1,2}(t)$ will decay exponentially[1] as

$$A_{1,2}(t) = A_{1,2}(0) \exp\left(-\frac{kr(x^*)}{P_{1,2}} t\right) \tag{14}$$

with different exponents for each of the two local minima, that (as we will show later) results in the exponential character of the residence time distributions for each of the two coexisting regimes. Indeed, the residence time distribution for the regime corresponding to the first local minimum can be expressed as (see, e.g., [48])

$$p_1(t) = -\int_{-\infty}^{x^*} \frac{\partial \rho_1(x,t)}{\partial t} dx, \tag{15}$$

while for the second local minimum, Eq. (15) takes the form

$$p_2(t) = -\int_{x^*}^{+\infty} \frac{\partial \rho_2(x,t)}{\partial t} dx. \tag{16}$$

Substituting Eqs. (5), (10), (11) and (14) into Eqs. (15) and (16), and taking into account the normalization conditions

$$\begin{aligned} \int_{-\infty}^{x^*} \rho_1(\xi,0)\,d\xi &= \int_{-\infty}^{x^*} A_1(0) r(\xi) d\xi = 1, \\ \int_{x^*}^{+\infty} \rho_2(\xi,0)\,d\xi &= \int_{x^*}^{+\infty} A_2(0) r(\xi)\,d\xi = 1, \end{aligned} \tag{17}$$

we obtain the following relations for the residence time distributions:

$$p_{1,2}(t) = \kappa_{1,2} \exp(-\kappa_{1,2} t), \tag{18}$$

where

$$\kappa_{1,2} = \frac{kr(x^*)}{P_{1,2}}, \tag{19}$$

i.e., in the regime of noise-induced intermittency the residence time distributions obey the exponential laws.

On the basis of the obtained relations Eqs. (18)and (19) and the definition of the mean value

$$T_{1,2} = \int_0^{+\infty} t\, p_{1,2}(t) dt \tag{20}$$

we obtain the relation for the mean residence times for each of the two coexisting regimes

$$T_{1,2} = \frac{1}{\kappa_{1,2}} = \frac{P_{1,2}}{kr(x^*)}. \tag{21}$$

Therefore, the analytical Eq. (18) for the residence time distributions in the regime of noise-induced intermittency can be written in the following form

$$p_{1,2}(t) = \frac{1}{T_{1,2}} \exp\left(-\frac{t}{T_{1,2}}\right). \tag{22}$$

Having substituted the explicit relations for the probabilities $P_{1,2}$ and stationary probability density $r(x^*)$ into Eq. (21) and taking into account that the boundary point $x^* \approx b$ for small b, we obtain the expressions for the mean residence times corresponding to the coexisting regimes as follows

$$\begin{aligned} T_1 &= \frac{L_1}{k} \exp\left[\frac{2}{D}\left(\frac{b^4}{4} + \frac{b^2}{2}\right)\right], \\ T_2 &= \frac{L_2}{k} \exp\left[\frac{2}{D}\left(\frac{b^4}{4} + \frac{b^2}{2}\right)\right], \end{aligned} \tag{23}$$

where the integrals

$$L_1 = \int_{-\infty}^{x^*} g(\xi)\,d\xi \quad \text{and} \quad L_2 = \int_{x^*}^{+\infty} g(\xi)\,d\xi \tag{24}$$

can be found numerically.

In the symmetric case ($b = 0$) the mean residence times T_1 and T_2 match each other, $T_1 = T_2 = T$. Moreover, as it has been shown in [49–51], they should coincide with the mean first passage time of the point of symmetry. Furthermore, the integrals (24) can be found in the explicit form allowing the analytical expression for the mean residence time

$$T = \frac{\pi}{4k} \exp\left(\frac{1}{4D}\right)\left[I_{-1/4}\left(\frac{1}{4D}\right) + I_{1/4}\left(\frac{1}{4D}\right)\right], \tag{25}$$

where $I_\alpha(x)$ is the modified Bessel function of the first kind.

Thus, in the regime of noise-induced intermittency the statistical characteristics of the residence time should obey Eqs. (22) and (23).

3. Examples of noise-induced intermittency

To verify our theoretical predictions we analyze numerically the behavior of three different bistable systems which exhibit noise-induced intermittency.

3.1. Bistable energy model

As the first example we consider the bistable energy system (1) given in Section 1 with the potential function Eq. (2) and

[1] It should be noted that in more general case (e.g., when the noise intensity is comparable or larger than the potential barrier height) the Eq. (12) is not valid, and solution can be found only numerically (see [44–47] for details).

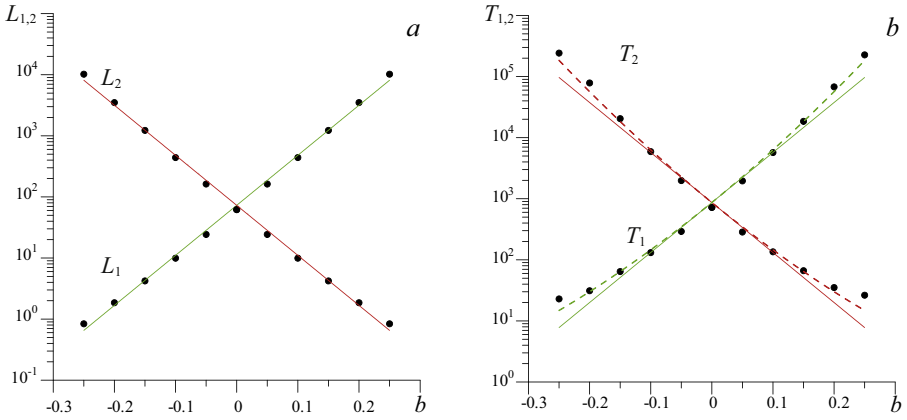

Fig. 2. (Color online) Dependencies of (a) integrals $L_{1,2}$ and (b) mean residence times $T_{1,2}$ for two coexisting regimes on criticality parameter b (dots) and their approximations by exponential laws Eqs. (26) and (28) (solid lines) and Eq. (27) (dashed lines). Parameters of approximations are (a) $C = 72.86$, $\alpha = 18.86$, (b) $K = 867$, $\alpha = 18.85$, $D = 0.1$.

noise intensity $D = 0.1$. Fig. 1(a) and (d) show the potential functions $U(x)$ for the symmetric ($b = 0$) and asymmetric ($b = 0.15$) cases. In the same Fig. 1(b,c,e and f) we plot the corresponding statistical distributions of the residence times for two coexisting regimes: in Fig. 1(b,e) for the left state $-\infty < x < x^*$, and in Fig. 1(c,f) for the right state $x^* < x < +\infty$. The results of the numerical simulations are marked by dots and triangles for two coexisting regimes, while the theoretical approximations using the exponential laws Eq. (22) with the parameters indicated in the caption, are represented by straight lines. An excellent agreement can be seen between the results of the numerical calculations and theoretical approximations for both the symmetric and asymmetric potentials; this demonstrates the validity of the developed theory.

As additional evidence for the correctness of the obtained results, we find the dependence of the mean residence time for each of the coexisting regimes, on the control parameter b. The analytical relation for such a dependence requires the calculation of the integrals $L_{1,2}$ (Eq. 24) for different values of the asymmetry parameter b. In Fig. 2(a) we plot these dependencies calculated numerically for both integrals (marked by dots) and their approximations (solid lines). It is clearly seen that the exponential laws fit these dependencies very well, i.e.

$$L_{1,2} = C\exp(\mp\alpha b) \tag{26}$$

with the constants $C = 72.86$ and $\alpha = 18.86$. Thus, the mean residence times for both coexisting regimes obey the following relation

$$T_{1,2} = K\exp(\pm\alpha b)\exp\left[\frac{2}{D}\left(\frac{b^4}{4} + \frac{b^2}{2}\right)\right], \tag{27}$$

where $K = C/k$ is constant.

Fig. 2(b) shows the numerically obtained dependencies of the mean residence times for two coexisting regimes (marked by dots) and their theoretical approximations by regularities Eq. (27) (dashed lines). The curve T_1 corresponds to the left state x_1, while the curve T_2 refers to the right state x_2. The approximation parameters are indicated in the caption. A very good agreement is clearly seen between the results obtained theoretically and numerically in almost the whole range of the considered values of the asymmetry parameter b.

It should be noted that for the small values of the asymmetry parameter b the exponential term $\exp\left[\frac{2}{D}\left(\frac{b^4}{4} + \frac{b^2}{2}\right)\right]$ in Eq. (27) is close to 1, and, therefore, the dependencies of the mean residence times can be approximated by the exponential law

$$T_{1,2} = K\exp(\mp\alpha b). \tag{28}$$

These dependencies are shown in Fig. 2(b) by straight solid lines. It is clearly seen that for $b \in [-0.15, 0.15]$ the theoretical curves Eqs. (27) and (28) almost coincide with each other, which allows the successful application of the same approximation Eq. (28) to the numerical data. For relatively large values of the asymmetry parameter b the numerically obtained data distants itself from the theoretical approximation curves by Eq. (28), meaning that the assumption at the derivation of regularity Eq. (28) cannot be applied anymore and, therefore, the initial theoretical law Eq. (27) must be used.

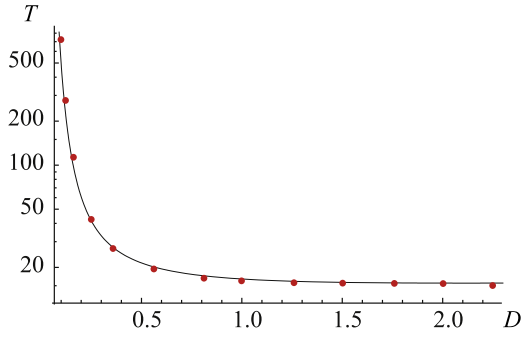

Fig. 3. (Color online) Dependence of mean residence time T on noise intensity D obtained for symmetrical case $b = 0$ numerically (dots) and theoretical prediction Eq. (25) (solid line). The ordinate axis is shown in log scale.

Finally, the deduced dependence of the mean residence time on the noise intensity Eq. (25) for the symmetrical case $b = 0$ is also in a good agreement with the results of the numerical calculations (see Fig. 3). The mean residence times obtained for different values of the noise intensity represented in Fig. 3 by dots are successfully fitted by the predicted theoretical curve Eq. (25) within the broad range of the parameter D.

Thus, for relatively small values of the asymmetry parameter b, the dependencies of the mean residence times for both coexisting regimes obey the exponential laws (28) in full agreement with our theoretical prediction, whereas for large values of b, the more sophisticated and more precise expression Eq. (27) should be used. For fixed values of the asymmetry parameter and noise intensity, the residence time distributions satisfy the exponential laws Eq. (22).

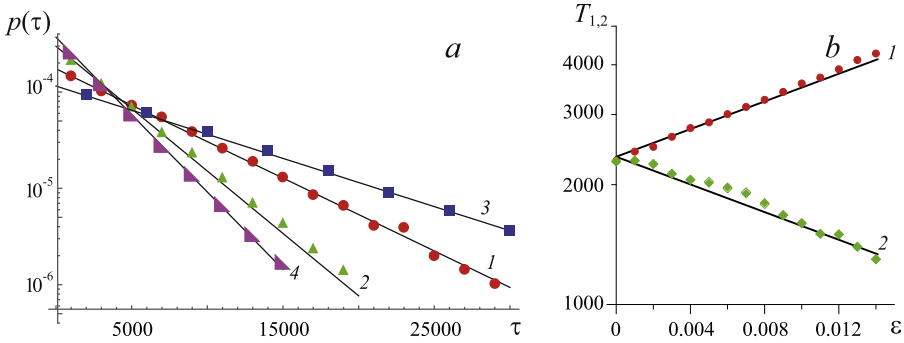

Fig. 4. (a) Residence time distributions of the system (29) for in-phase (curves 1,3) and anti-phase (curves 2,4) states for the fixed values of the control parameters ($\lambda = 1.05$, $D = 0.06$, $\varepsilon = 0.002$ for curves 1,2, $\varepsilon = 0.012$ for curves 3,4) and their theoretical approximations by the regularity (22). Theoretical curves are shown by solid lines, numerically obtained data are marked by point. Vertical axis is shown in logarithmic scale. (b) Dependencies of the mean residence times for in-phase (curve 1) and anti-phase (curve 2) states on the coupling parameter ε and their theoretical approximations by regularity (27). Theoretical curves are shown by solid lines, numerically obtained data are marked by point. Vertical axis is shown in logarithmic scale. Parameters of approximations have been selected as follows: $K = 2350$, $\alpha = 40$.

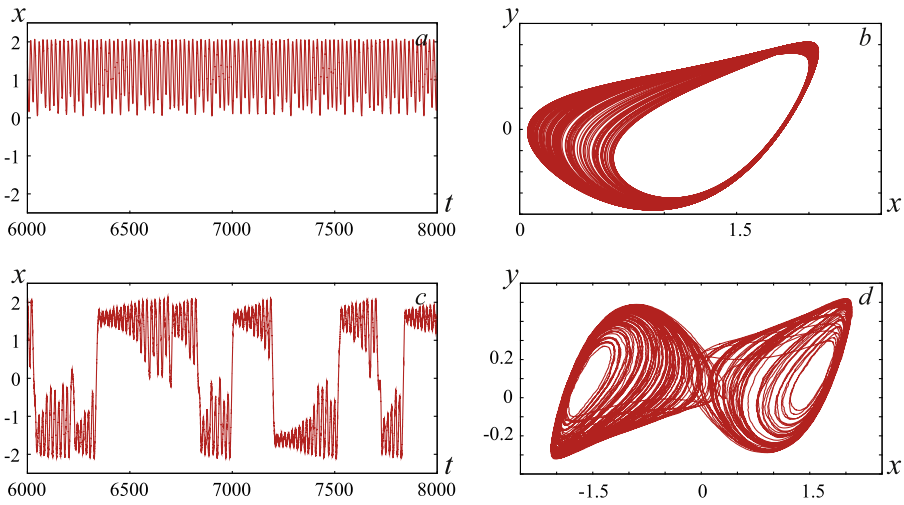

Fig. 5. Time realizations (a,c) of the change of voltage on nonlinear element of Chua generator (30) and phase portraits (b,d) of such system for different values of the noise intensity: (a,b) $D = 0.0$, (c,d) $D = 1.0$.

3.2. Coupled logistic maps

In the next example we consider two mutually dissipatively coupled logistic maps studied in [52,53] with multiplicative noise. It should be noted that just the multiplicative noise plays an essential role in biological systems (see, e.g. [54–56]). The system under study is given by

$$\begin{aligned} x_{n+1} &= f(x_n, \lambda) + \varepsilon(f(y_n, \lambda) + Df(\xi_n, 1) - f(x_n, \lambda)), \\ y_{n+1} &= f(y_n, \lambda) + \varepsilon(f(x_n, \lambda) + Df(\xi_n, 1) - f(y_n, \lambda)), \end{aligned} \tag{29}$$

where $f(x, \lambda) = \lambda - x^2$, ξ_n is a noise term with zero mean value, D is a noise intensity, λ is a control parameter, ε is a coupling strength. As it has been shown in [52], for the certain values of the control parameters logistic maps under study can demonstrate both in-phase and anti-phase states depending on the choice of initial conditions. If the additional noise term is added in the system, i.e. $D > 0$, as in the case of energy model (1) and (2), the switching between the in-phase and anti-phase states would be observed. As we have shown in [53], such switching can be characterized by the parameter $z_n = x_{2n}$ at condition $y_{2n} < 0.6$, at that the distribution of z_n should be described by Eq. (2). In other words, the appearance of the noise-induced intermittency in the system (29) allows us to apply the theory developed in Section 2 to the system under study. In Fig. 4 we show the numerically obtained distributions of the residence times corresponding to the in-phase and anti-phase regimes (a) and dependencies of their mean residence times on the control parameter ε (b) as well as their theoretical approximations by the regularities Eqs. (22) and (27), respectively. It is clearly seen a good agreement between the theoretically and numerically obtained data for both regimes observed in the system.

3.3. Bistable Chua generator

As the last example we consider bistable generator with chaotic dynamics proposed by Chua et al. [57]. The system under study is given by

$$\begin{aligned} \dot{x} &= y - x - h(x) + D\xi, \\ \dot{y} &= \alpha^{-1}(x - y + z), \\ \dot{z} &= -\delta(y + \rho z), \end{aligned} \tag{30}$$

where $\xi(t)$ is random Gaussian process with zero mean and unit variance, D is an intensity of noise influence, variable x characterises the change of voltage on nonlinear elements of the system, variable y corresponds to the changes of voltage on capacitors in oscillatory circuit, whereas the variable z characterizes the changes of inductor current [58]. As characteristic of nonlinear element the third-degree polynomial has been used [58]:

$$h(x) = -1.25x - 0.1x^3. \tag{31}$$

The constant coefficients have been selected as follows: $\alpha = 9$, $\delta = 9$. The dissipation parameter ρ has been chosen to be $\rho = 0.01$,

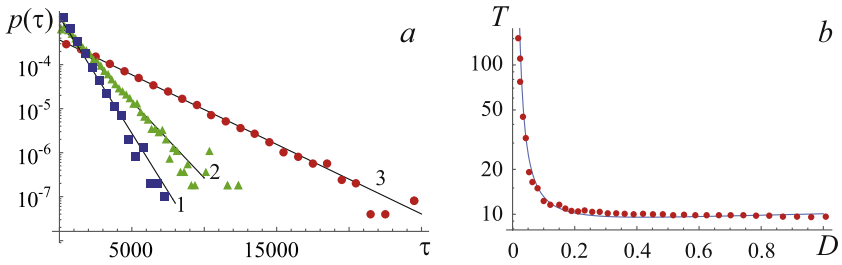

Fig. 6. (*a*) Residence time distributions of Chua generator (30) near the first stable state and their theoretical approximations by the regularity (22): 1 — $D = 0.26$, 2 — $D = 0.32$, 3 — $D = 0.37$. (*b*) Dependence of the mean residence time for the system (30) near the first stable state on the noise intensity and its theoretical approximation by the regularity (27) for $k = 0.318$. Theoretical curves in Fig. 6(a,b) are shown by solid lines, numerically obtained data are marked by points. Vertical axes are shown in logarithmic scale .

that corresponds to the realization of autonomous oscillations in the system under study in the one from two basins of attraction depending on the choice of initial conditions. Fig. 5(a) illustrates such situation in the case when the external noise amplitude D is equal to zero, i.e. the system under study remains near the one stable state. The phase portrait of Chua generator in such case is shown in Fig. 5(b). At that, if the noise of high enough amplitude influences on the system, the sequential transitions from the one stable state to the other one would be observed. In other words, in such case in Chua generator (30) the noise-induced intermittency would be observed. Such situation is illustrated in Fig. 5(c) where it is clearly seen that the system alternately switches from the one stable state to the other one. In Fig. 5(d) the phase portrait of the system in such case is shown.

Then we have analyzed the statistical characteristics of noise-induced intermittency in the system under study (30). Due to the symmetry of the chaotic attractor, we have restricted by the consideration of such characteristics near the only one stable state. In Fig. 6(a) the residence time distributions corresponding to the first stable state of Chua generator for the fixed values of the control parameters are shown. The numerically obtained data are marked by points, their theoretical approximations by the regularity (22) are shown by solid lines. Moreover, we have also obtained the dependence of the mean residence time for the same stable state of the system (30) on the noise intensity. It is shown in Fig. 6(b) by points, its theoretical approximation by the regularity (25) is specified by solid line. It is clearly seen from Fig. 6(a,b) that the theoretical predictions and numerically obtained data are in a good agreement with each other that allows us to apply the proposed theory to the flow systems demonstrating chaotic dynamics.

4. Conclusion

In the present paper we have proposed the theory of noise-induced intermittency in bistable dynamical systems. We have shown that the residence time distributions for every coexisting regime obey the exponential laws. The exponential law has also been observed for the dependencies of the mean residence times on the criticality parameter. The validity of the proposed theory has been demonstrated with the help of the bistable generic energy model, coupled logistic maps and bistable Chua generator.

It should be noted that despite of the fact that the most part of results has been obtained for the Gaussian source of noise, they remain qualitatively the same for other sources of noise added in the systems under study that is quite typical for nonlinear systems including chaotic ones (see, e.g., [20,59–63]).

Authors thank Prof. Alexander N. Pisarchik for useful comments and discussions. This work has been supported by Russian Foundation for Basic Research (project no. 16-32-60078).

References

[1] Berge P, Pomeau Y, Vidal C. Order within chaos. New York: John Wiley and Sons; 1984.
[2] Manneville P, Pomeau Y. Intermittency and the Lorenz model. Phys Lett A 1979;75:1.
[3] Grebogi C, Ott E, Romeiras FJ, Yorke JA. Critical exponents for crisis-induced intermittency. Phys Rev A 1987;36(11):5365–80.
[4] Pikovsky AS, Osipov GV, Rosenblum MG, Zaks M, Kurths J. Attractor–repeller collision and eyelet intermittency at the transition to phase synchronization. Phys Rev Lett 1997;79(1):47–50.
[5] Boccaletti S, Valladares DL. Characterization of intermittent lag synchronization. Phys Rev E 2000;62(5):7497–500.
[6] Hramov AE, Koronovskii AA. Intermittent generalized synchronization in unidirectionally coupled chaotic oscillators. Europhys Lett 2005;70(2):169–75.
[7] Hramov AE, Koronovskii AA, Kurovskaya MK, Boccaletti S. Ring intermittency in coupled chaotic oscillators at the boundary of phase synchronization. Phys Rev Lett 2006;97:114101.
[8] Moskalenko OI, Koronovskii AA, Shurygina SA. Intermittent behavior on the boundary of the noise-induced synchronization. Tech Phys 2011;56(9):1369–72.
[9] Hramov A, Koronovskii A, Kurovskaya MK. Intermittent behavior near the synchronization threshold in system with fluctuating control parameter. Europhys Lett 2014;105:50003.
[10] Kim CM, Yim GS, Ryu JW, Park YJ. Characteristic relations of type-iii intermittency in an electronic circuit. Phys Rev Lett 1998;80(24):5317–20. doi:10.1103/PhysRevLett.80.5317.
[11] Velazquez JLP, et al. Type III intermittency in human partial epilepsy. Eur J Neurosci 1999;11:2571–6.
[12] Kiss IZ, Hudson JL. Phase synchronization and suppression of chaos through intermittency in forcing of an electrochemical oscillator. Phys Rev E 2001;64(4):046215.
[13] Boccaletti S, Allaria E, Meucci R, Arecchi FT. Experimental characterization of the transition to phase synchronization of chaotic CO_2 laser systems. Phys Rev Lett 2002;89(19):194101.
[14] Cabrera JL, Milton JG. On–off intermittency in a human balancing task. Phys Rev Lett 2002;89(15):158702.
[15] Hramov AE, Koronovskii AA, Midzyanovskaya IS, Sitnikova E, Rijn CM. On–off intermittency in time series of spontaneous paroxysmal activity in rats with genetic absence epilepsy. Chaos 2006;16:043111.
[16] Sitnikova E, Hramov AE, Grubov VV, Ovchinnkov AA, Koronovsky AA. On–off intermittency of thalamo-cortical oscillations in the electroencephalogram of rats with genetic predisposition to absence epilepsy. Brain Res 2012;1436:147–56.
[17] Dubois M, Rubio MA, Bergé P. Experimental evidence of intermittencies associated with a subharmonic bifurcation. Phys Rev Lett 1983;51:1446–9.
[18] Heagy JF, Platt N, Hammel SM. Characterization of on–off intermittency. Phys Rev E 1994;49(2):1140–50.
[19] Hramov AE, Koronovskii AA, Moskalenko OI, Zhuravlev MO, Ponomarenko VI, Prokhorov MD. Intermittency of intermittencies. Chaos 2013;23(3):033129.
[20] Moskalenko OI, Koronovskii A, Hramov A, Zhuravlev M, Levin Y. Cooperation of deterministic and stochastic mechanisms resulting in the intermittent behavior. Chaos Solitons Fractals 2014;68:58–64.
[21] Koronovskii AA, Hramov AE, Grubov VV, Moskalenko OI, Sitnikova E, Pavlov AN. Coexistence of intermittencies in the neuronal network of the epileptic brain. Phys Rev E 2016;93:032220. doi:10.1103/PhysRevE.93.032220.
[22] Chen JY, Wong KW, Zheng HY, Shuai JW. Intermittent phase synchronization of coupled spatiotemporal chaotic systems. Phys Rev E 2001;64(1):016212.
[23] Pisarchik AN, Jaimes-Reategui R, Villalobos-Salazar JR, García-López JH, Boccaletti S. Synchronization of chaotic systems with coexisting attractors. Phys Rev Lett 2006;96:244102. doi:10.1103/PhysRevLett.96.244102.
[24] Pisarchik AN, Jaimes-Reategui R, Sevilla-Escoboza R, Huerta-Cuellar G. Multistate intermittency and extreme pulses in a fiber laser. Phys Rev E 2012;86(5):056219.
[25] Sevilla-Escoboza R, Buldu JM, Pisarchik AN, Boccaletti S, Gutierrez R. Synchronization of intermittent behavior in ensembles of multistable dynamical systems. Phys Rev E 2015;91:032902.

[26] Arecchi FT, Badii R, Politi A. Generalized multistability and noise-induced jumps in a nonlinear dynamical system. Phys Rev A 1985;32:402–8. doi:10.1103/PhysRevA.32.402.
[27] Wiesenfeld K, Hadley P. Attractor crowding in oscillator arrays. Phys Rev Lett 1989;62:1335–8. doi:10.1103/PhysRevLett.62.1335.
[28] Kraut S, Feudel U. Multistability, noise, and attractor hopping: the crucial role of chaotic saddles. Phys Rev E 2002;66:015207. doi:10.1103/PhysRevE.66.015207.
[29] Pisarchik AN, Jaimes-Reategui R, Sevilla-Escoboza R, Huerta-Cuellar G, Taki M. Rogue waves in a multistable system. Phys Rev Lett 2011;107:274101.
[30] Hramov AE, Koronovskii AA, Moskalenko OI, Zhuravlev MO, Jaimes-Reategui R, Pisarchik AN. Separation of coexisting dynamical regimes in multistate intermittency based on wavelet spectrum energies in an erbium-doped fiber laser. Phys Rev E 2016;93:052218. doi:10.1103/PhysRevE.93.052218.
[31] Lai YC, Grebogi C. Intermingled basins and two-state on-off intermittency. Phys Rev E 1995;52:R3313–16.
[32] Pisarchik AN, Pinto-Robledo VJ. Experimental observation of two-state on–off intermittency. Phys Rev E 2002;66:027203.
[33] Roy R, Short R, Durnin J, Mandel L. First-passage-time distributions under the influence of quantum fluctuations in a laser. Phys Rev Lett 1980;45:1486–90. doi:10.1103/PhysRevLett.45.1486.
[34] Hänggi P, Mroczkowski T, Moss F, McClintock PVE. Bistability driven by colored noise: theory and experiment. Phys Rev A 1985;32:695–8. doi:10.1103/PhysRevA.32.695.
[35] Hänggi P, Talkner P, Borkovec M. Reaction-rate theory: fifty years after Kramers. Rev Mod Phys 1990;62:251–341. doi:10.1103/RevModPhys.62.251.
[36] Mackey MC, Milton JG. A deterministic approach to survival statistics. J Math Biol 1990;28(1):33–48. doi:10.1007/BF00171517.
[37] Kramers HA. Brownian motion in a field of force and the diffusion model of chemical reactions. Physica 1940;7(4):284–304. doi:10.1016/S0031-8914(40)90098-2.
[38] Gammaitoni L, Hänggi P, Jung P, Marchesoni F. Stochastic resonance. Rev Mod Phys 1998;70(1):223–87.
[39] Moreno-Bote R, Rinzel J, Rubin N. Noise-induced alternations in an attractor network model of perceptual bistability. J Neurophysiol 2007;98:1125–39.
[40] Pisarchik AN, Jaimes-Reategui R, Magallón-Garcia AD, Castillo-Morales O. Critical slowing down and noise-induced intermittency in bistable perception: bifurcation analysis. Biol Cybern 2014;108(4):397–404.
[41] Semenov V, Neiman AB, Vadivasova TE, Anishchenko VS. Noise-induced transitions in a double-well oscillator with nonlinear dissipation. Phys Rev E 2016;93:052210. doi:10.1103/PhysRevE.93.052210.
[42] Poston T, Stewart I. Catastrophe theory and its applications. Pitman; 1978.
[43] Runnova A, Hramov AE, Grubov V, Koronovsky A, Kurovskaya MK, Pisarchik AN. Theoretical background and experimental measurements of human brain noise intensity in perception of ambiguous images. Chaos Solitons Fractals 2016;93:201–6.
[44] Nikitenkova S, Pankratov AL. Nondecay probability of the “correct” state of a memory cell: analytic approach versus numeric simulation. Phys Rev E 1998;58:6964–7. doi:10.1103/PhysRevE.58.6964.
[45] Pankratov AL. Time evolution of averages in dynamical systems driven by noise. Phys Lett A 1999;255(1):17–22. doi:10.1016/S0375-9601(99)00164-4.
[46] Antonov AA, Pankratov AL, Yulin AV, Mygind J. Influence of thermal fluctuations on cherenkov radiation from fluxons in dissipative Josephson systems. Phys Rev B 2000;61:9809–19. doi:10.1103/PhysRevB.61.9809.
[47] Malakhov AN, Pankratov AL. Evolution times of probability distributions and averages-exact solutions of the Kramers problem. Adv Chem Phys 2002;121:357–438.
[48] Koronovskii AA, Hramov AE. Type-II intermittency characteristics in the presence of noise. Eur Phys J B 2008;62:447–52.
[49] Malakhov AN, Pankratov AL. Influence of thermal fluctuations on time characteristics of a single Josephson element with high damping exact solution. Physica C Supercond 1996;269(1):46–54. doi:10.1016/0921-4534(96)00426-1.
[50] Malakhov AN. Time scales of overdamped nonlinear Brownian motion in arbitrary potential profiles. Chaos Interdiscip J Nonlinear Sci 1997;7(3):488–504. doi:10.1063/1.166220. ArXiv: https://doi.org/10.1063/1.166220.
[51] Pankratov AL. On certain time characteristics of dynamical systems driven by noise. Phys Lett A 1997;234(5):329–35. doi:10.1016/S0375-9601(97)00599-9.
[52] Astakhov VV, Bezruchko BP, Gulyaev Y, Seleznev EP. Multistable states of dissipatively coupled Feigenbaum's systems. Sov Tech Phys Lett 1989;15(3):60–5.
[53] Zhuravlev MO, Koronovskii AA, Moskalenko OI, Hramov AE. Statistical characteristics of noise-induced intermittency in multistable systems. Izvestiya VUZ Appl Nonlinear Dyn 2018;26(1):80–9.
[54] La Barbera A, Spagnolo B. Spatio-temporal patterns in population dynamics. Phys A Stat Mech Appl 2002;314(1):120–4. doi:10.1016/S0378-4371(02)01173-1. Horizons in Complex Systems.
[55] Ciuchi S, de Pasquale F, Spagnolo B. Nonlinear relaxation in the presence of an absorbing barrier. Phys Rev E 1993;47:3915–26. doi:10.1103/PhysRevE.47.3915.
[56] Valenti D, Fiasconaro A, Spagnolo B. Pattern formation and spatial correlation induced by the noise in two competing species. Acta Phys Pol B 2004;35(4):1481–9.
[57] Chua LO, Komuro M, Matsumoto T. The double scroll family. IEEE Trans Circuits Syst 1986;33(11):1073–118.
[58] Kalyanov E. Features of induced synchronization of a bistable oscillator with chaotic dynamics. Tech Phys Lett 2011;37(11):1042–5.
[59] Kye WH, Kim CM. Characteristic relations of type-i intermittency in the presence of noise. Phys Rev E 2000;62(5):6304–7.
[60] Anishchenko VS, Vadivasova TE, Strelkova GI. Instantaneous phase method in studying chaotic and stochastic oscillations and its limitations. Fluct Noise Lett 2004;4(1):L219–29.
[61] Hramov AE, Koronovskii AA, Kurovskaya MK, Ovchinnikov AA, Boccaletti S. Length distribution of laminar phases for type-I intermittency in the presence of noise. Phys Rev E 2007;76(2):026206.
[62] Dubkov AA, Spagnolo B. Verhulst model with lévy white noise excitation. Eur Phys J B 2008;65(3):361–7. doi:10.1140/epjb/e2008-00337-0.
[63] Augello G, Valenti D, Spagnolo B. Non-Gaussian noise effects in the dynamics of a short overdamped Josephson junction. Eur Phys J B 2010;78(2):225–34. doi:10.1140/epjb/e2010-10106-1.